

# Chemical state analysis of magnesium-supported Ziegler-Natta catalyst by soft X-ray emission spectrometer (SXES) after contact with alkyl aluminum

Masayoshi Saito<sup>1,\*</sup>, Hiroshi Kashimura<sup>1</sup>, Takuo Kataoka<sup>1</sup>, Masahide Murata<sup>2</sup>,  
Yusuke Sakuda<sup>3</sup>, Hiroyuki Yamada<sup>3</sup>, Hideyuki Takahashi<sup>3</sup>

<sup>1</sup>Analysis Center, Toho Titanium Co., LTD., 3-3-5, Chigasaki Chigasaki-City, Kanagawa, 253-8510, Japan

<sup>2</sup> Former Toho Titanium Co., LTD.,

<sup>3</sup>JEOL Ltd., 3-1-2 Musashino, Akishima, Tokyo 196-8558, Japan

\*Corresponding Author – E-mail: m-saito@toho-titanium.co.jp

Telephone number: +81-467-87-2812

Fax number: +81-467-83-0213

Received: 5 January 2024, Accepted: 1 April 2024

DOI: 10.22063/POJ.2024.3557.1292

## ABSTRACT

This report is on the characterization of active Ti center in heterogeneous Ziegler-Natta catalysts with Soft X-ray Emission Spectrometer (SXES). Since titanium in the catalyst has various chemical bonds, it is important to grasp the chemical bond state. The outermost shell electrons are very important for understanding the chemical bond state. SXES is the only method that can easily observe outermost shell electrons with current analytical instruments. Here, a co-milled solid of MgCl<sub>2</sub>, TiCl<sub>4</sub>, and Phthalate was used as a catalyst precursor, and three types of catalysts with significantly different catalytic activity levels were synthesized by changing the subsequent preparation process. The correlation between catalytic activity and the signal shape of L $\alpha$ , $\beta$  emission, which is the outermost shell electron of Ti in SXES analysis, was investigated. L $\alpha$ , $\beta$  emission was detected as broad signal. It could be observed that the high active catalyst had relatively strong signal intensity at the high energy side.

The shape changes were also checked when the catalyst solids were treated by triethylaluminium. By this treatment, the relative intensity of the high energy side signal was further enhanced, suggesting that triethylaluminium treatment induced the elimination of inactive Ti from the catalyst solid. By comparing with the solid <sup>13</sup>C-NMR analyses data of the Ziegler-Natta catalyst described in our previous report, the high energy side signal of Ti L $\alpha$ , $\beta$  in SXES results implies the relationship with the NMR results for carbonyl function.

**Keywords:** Ziegler-Natta catalyst; propene polymerization; soft X-ray emission spectrometer (SXES); field emission scanning electron microscope (FE-SEM); polymerization activity; outermost shell electrons of titanium.

## INTRODUCTION

It is well known that the Ziegler-Natta catalyst is used for the polymerization of olefins such as ethylene and propylene. The basic configuration of this catalyst is to use a Ti chloride component

as the main catalyst and alkyl aluminum as the co-catalyst. Ti is activated by alkyl aluminum to form an active species. The fierce development research has been conducted to improve the performance of the catalyst.

The magnesium chloride-supported catalyst shows dramatically higher activity than the initial titanium trichloride catalyst. Taking advantage of this ultra-high activity, it has now become the mainstream catalyst for the industrial manufacturing of polyethylene and polypropylene [1-5]. In addition, in the production of polypropylene, the high stereo regularity of polymer is another essential requirement, and in order to realize it, the development of electron donating compounds that coexist in the catalytic system has also progressed.

In parallel with such industrial production technological innovation, basic research has been conducted to understand the factors of high performance. For example, we were able to see the electron characteristics of titanium atom in an ethylene polymerization catalyst for the first time in the world by using high-field solid-state NMR [6]. The catalyst was simple as a configuration in which  $\text{TiCl}_4$  was supported on  $\text{MgCl}_2$ . It was observed that the NMR signal of Ti shifted toward to the high magnetic field direction, suggesting that the high catalytic activity shall appear when the electron density of Ti is high. On the other hand, unfortunately, a solid-state NMR spectrum could not obtain in a catalyst for polypropylene polymerization containing an electron donor. The reasons for this are considered to be as follows. That is, since the titanium element is a quadrupole nucleus, the electric field gradient in the material is overwhelmingly larger than other interactions in a structure without symmetry. Therefore, in nuclei with quadrupole moments, the relaxation time is shortened because the relaxation is almost dominated by the quadrupole nuclear interaction. When the electron donor is unevenly coordinated on magnesium chloride, the relaxation time is shortened to 1 second or less because it has a structure without symmetry. As the relaxation time becomes shorter, the waveform suffers from an oscillating phenomenon (acoustic ringing) due to the resonance of the NMR pulse (radio wave), and this effect makes observation difficult [7-9]. Thus, since it has been difficult to directly observe the electronic state of Ti for propylene polymerization catalysts at the level of analytical technology, analysis focusing on organic electron donating compounds coexisting in catalysts that are easy to track has been conducted. Here, infrared spectroscopy, thermal analysis, or solid-state NMR analysis have been performed. Based on the analytical results, a structure in which titanium and electron donors in the catalyst are individually supported on magnesium chloride has been proposed [10-31]. This strongly suggests that the electronic state of the active titanium species is affected by the support magnesium chloride in the propylene polymerization catalyst as well as the ethylene polymerization catalyst. In fact, based on kinetic studies, the relationship between charge density and polymerization activity of active Ti has been discussed [11,12,14]. In addition, studies have been conducted to infer the structure of the active species on the surface of  $\text{MgCl}_2$ . For example, quantum chemical calculations have been performed using a model in which Ti halide is bonded to the surface defects of various crystal

planes of  $\text{MgCl}_2$  [19,20,25-27,30,31]. Recently, an attempt has been made to identify the crystal backbone around the Ti species, which may exist on the surface of  $\text{MgCl}_2$ , by predicting the X-ray Absorption Near Edge Structure (NEXAFS) spectral from the DFT calculation of the model structure of the surface-active species. And the calculation results were compared with the actual measured signal [26,28,30]. It has been confirmed that there is a species in the catalyst solid in which the mono-metallic  $\text{Ti}^{4+}$  species is supported on the (001) crystal plane of surface defect of  $\text{MgCl}_2$ . Furthermore, by activation with organoaluminum, Ti is reduced to trivalent, and it has been reported that at least  $\text{Ti}^{3+}$  species having an alkyl group are active for ethylene polymerization. This is excellent example of how advances in spectroscopic instruments have contributed greatly to the understanding of polymerization catalytically active species.

On the other hand, the actual  $\text{MgCl}_2$ -supported catalyst has an easy change in performance such as activity depending on the preparation method and preparation conditions. Furthermore, it is very obvious that the active species in the catalyst are heterogeneous. The clear evidence on the heterogeneity of the active sites is the broad molecular weight distribution of the produced polymer. If this heterogeneity can be understood as the distribution of the properties of Ti species in the catalyst, we will be able to further approach the essence of the active species.

In recent years, Soft X-ray Emission Spectrometer (SXES) has been developed [32-38]. Since this instrument has an energy resolution of more than two orders of magnitude higher than Energy Dispersive x-ray Spectrometer (EDS), it is easy to obtain information on element-specific outermost shell electrons [39] and chemical bonding states. In fact, when we analyzed the titanium element in the magnesium chloride-supported propylene polymerization catalyst using SXES, we succeeded to observe the tendency of Ti  $L\alpha,\beta$  emission and the relation with their catalytic activity. Furthermore, when compared with the charge density parameter of carbonyl function based on NMR data and the catalytic performance, it could be found the correlation, which the spectral polarization to higher energy side signal of  $L\alpha,\beta$  emission spectra of Ti seemed to provide the high active catalyst site[40,41].

In this study, SXES analysis of conventional titanium trichloride catalysts was performed and compared with the results of magnesium chloride supported catalysts reported earlier. And SXES analysis of activated Ti species was also attempted by using magnesium chloride supported catalysts after the contact with alkyl aluminum.

## **EXPERIMENTAL**

### **$\text{MgCl}_2$ supported catalyst solid preparations**

#### *Catalyst A (Cat. A)*

632mmol of  $\text{MgCl}_2$  (surface area determined by BET method was  $11\text{m}^2/\text{g}$ ), 36mmol of  $\text{TiCl}_4$ , and

49mmol of di n-butyl phthalate (DBP) were introduced to a stainless vibration mill pot in which 50 balls of 25mm $\phi$  were charged. 48 h co-grinding was performed at room temperature. 30 g of the co-grinding solid was transferred to a 300 cm<sup>3</sup> volume glass flask fitted with mechanical agitation. The solid was washed with n-heptane at 40°C until free TiCl<sub>4</sub> had actually disappeared. (Ti content in washing solvent was monitored by ordinary calorimetry analysis.) Solid catalyst was obtained after drying under vacuum. Ti content of the catalyst was 2.5 wt%.

#### *Catalyst B (Cat. B)*

20 g of Cat. A and 200mL of toluene were charged into a 300 cm<sup>3</sup> volume glass flask fitted with mechanical agitation. Under agitation, the slurry was heated to 90°C and kept for 5min. The solution phase was separated out by decantation at 90°C. Successively, the solid part was washed with n-heptane at 40°C until toluene solvent was sufficiently exchanged by heptane. Solid catalyst was obtained after drying under vacuum. Ti content of the catalyst was 1.3 wt%.

#### *Catalyst C (Cat. C)*

10 g Cat. B, 20mL of TiCl<sub>4</sub>, and 80mL of toluene were introduced into a 300 cm<sup>3</sup> volume glass flask fitted with mechanical agitation. Under agitation, the slurry was heated to 100°C and kept for 120min. The solution phase was separated out by decantation at 100°C. Successively, the solid part was washed with n-heptane at 40°C until extracted TiCl<sub>4</sub> content reached zero. Solid catalyst was obtained after drying under vacuum. Ti content of the catalyst was 2.1 wt %.

### **Reference sample preparation**

#### *Alkyl aluminum (triethylaluminum) treatment of MgCl<sub>2</sub> supported catalyst*

Cat. A, B, and C were treated by triethylaluminum, respectively, to use SXES characterization. 10 g of each catalyst and 100 mL of n-heptane were added to a three-mouth flask provided with a nitrogen-substituted agitator. After addition, stirring in the flask and confirming that the catalyst was uniformly dispersed, triethylaluminum was added 5 times the titanium molar ratio in the catalyst. After addition, treatment was performed at room temperature for 1 hour. Finally, after washing with n-heptane, the catalyst that became black was vacuum-dried.

The catalytic activity of each triethylaluminum treated solids was immediately evaluated just after the solid preparation. The polymerization procedure was shown in the following session. And in order to avoid the alternation / deactivation of the solid, the remaining samples were stored at -20°C until to use for SXES characterization.

Hereafter, the triethylaluminum treated solids are described as Cat. A (Al), Cat. B (Al), and Cat. C (Al), respectively.

### *TiCl<sub>4</sub> DBP Complex*

A 1000 cm<sup>3</sup> three-necked flask was used for the reaction by connecting mechanical agitation and a dropping funnel. 200mL of n-heptane and 0.5mol of DBP were charged to the flask and the solution was heated at 40 °C. To the solution, 0.5mol of TiCl<sub>4</sub> was added dropwise slowly. After the completion of TiCl<sub>4</sub> addition, the reaction continued at 40 °C for 2 h. The precipitated solid was washed with n-heptane. Yellowish powder was obtained by vacuum drying. The powder composition was determined as TiCl<sub>4</sub>:DBP = 1:1.09 based on Ti content measurement.

### *MgCl<sub>2</sub>/TiCl<sub>4</sub> Co-Grinding Catalyst*

632mmol of MgCl<sub>2</sub> (surface area determined by BET method was 11m<sup>2</sup>/g), and 36mmol of TiCl<sub>4</sub> were introduced into a stainless vibration mill pot in which 50 balls of 25mm $\phi$  were charged. 48 h co-grinding was performed at room temperature. 10 g of the co-grinding solid was transferred to a 300 cm<sup>3</sup> volume glass flask fitted with mechanical agitation. The solid was washed with n-heptane at 40 °C. Solid catalyst was obtained after drying under vacuum. Ti content of the catalyst was 4.3 wt.%.

### *Synthesis conditions of titanium trichloride catalyst*

150 mL of n-heptane and 40 mL of titanium tetrachloride were added to a three-mouth flask with an internal volume of 1000 mL that was sufficiently nitrogen substituted. The liquid temperature was kept at 0°C, and a mixture of 150 mL of n-heptane and 45 mL of di-ethyl aluminum chloride was added dropwise for 4 hours. After completion of dropping, stirring was performed at the same temperature for 30 minutes, then the internal temperature was raised to 65°C for 1 hour, and then stirred for 1 hour. 150 mL of n-heptane at 40°C. was added and washed three times. Finally, a catalyst was obtained by heat treatment drying at 60°C for 1 hour.

## **Propene polymerization procedure**

### *Propene polymerization conditions with MgCl<sub>2</sub> supported catalyst*

2liter autoclave bulk polymerization, Al/Ti=500, Al/Donor=10, Ti=0.00264 mmol, External donor = CMDMSi, H<sub>2</sub> = 1.5NL, Liquid propylene=1.4 L, Pre-polymerization=20°C-5min., Main polymerization = 70°C-60 min.

The triethylaluminium treated solids were also evaluated by propylene polymerization tests under the equivalent conditions above.

### *Propene polymerization conditions with titanium trichloride catalyst*

500 mL of n-heptane is added to a stainless-steel autoclave with an internal volume of 2000 mL, and the temperature is raised to 70 °C after introducing 0.8 g of the above catalyst and 0.8 g of diethyl aluminum chloride, Polymerization was performed for 2 hours while supplying under a

pressure of propylene partial pressure of 0.4 MPa. After 2 hours, the propylene supply was stopped, the pressure was returned to normal pressure, ethanol was added into the autoclave, and stirred for 30 minutes. In order to quench the catalyst in the obtained powder, it was washed with 1 liter glass hydrochloric acid and ethanol containing a stir bar for 30 minutes, then washed with distilled water until the solvent became neutral, and finally dried under reduced pressure to obtain a solid polymer.

### **Characterization of Catalysts**

#### *SXES*

X-ray spectral analysis was performed by using SS-94040SXSER (SXES-ER) manufactured by JEOL Ltd.

In order to check the resolution sensitivity of SXES, MgCl<sub>2</sub>-Supported TiCl<sub>4</sub> catalyst was evaluated and compared by SXES and EDS. The details of the instruments used were as follows; SXES measurement was performed with JS300N of SXES-ER installed in the SEM machine (JSM-7200F manufactured by JEOL Ltd.) under the conditions of the accelerating voltage:5 kV, probe current:20 nA, exposure time:30 seconds, and accumulation:20.

SXES measurement of TiCl<sub>3</sub> catalyst was conducted with JS300N of SXES-ER installed in the EPMA machine (JXA-iHP200F manufactured by JEOL Ltd.) under the conditions of the accelerating voltage; 5 kV, probe current; 100 nA, exposure time; 60 seconds, accumulation; 10 times.

All preparation process was conducted under nitrogen inert atmosphere.

### **RESULTS AND DISCUSSION**

In the Ziegler-Natta catalyst, it is essential to use organoaluminium for the formation of active Ti species. For example, in a MgCl<sub>2</sub>-supported catalyst prepared with TiCl<sub>4</sub>, the tetravalent Ti is reduced by adding organoaluminium, and some part of trivalent Ti species generated work as the polymerization active centers[13]. To check the fundamentals of the effect of organoaluminium on the supported catalyst characteristic change, we first confirmed the titanium content in the catalyst before and after contact with triethylaluminium. The test results are shown in Table 1. The titanium content in the MgCl<sub>2</sub> supported catalysts decreased by the contact with triethylaluminium as the general manner. This is thought to be caused by the removal of titanium elements, which are weakly interact with MgCl<sub>2</sub> surface, by a strong reducing power of triethylaluminium.

This result gave us the attractive expectation to challenge SXES analysis of the catalyst solid treated by organoaluminium, since the influence of noise derived from inert Ti shall be reduced, and the electronic information of the active Ti species may be more emphasized and observed.

Figure1 shows the SXES measurement results of Cat.C before and after contact with triethylaluminium.

In both charts, several signals were observed from 370.0 eV to 490.0 eV energy ranges. The signal assignments are indicated in the chart of the before contacting with triethylaluminium. It could be able to observe Ti  $L\ell$ , and Ti  $L\alpha,\beta$  (influenced with the outermost shell electrons of titanium) signals, and Mg  $K\alpha$  (3rd order) in the  $MgCl_2$ -supported catalyst. The schematic diagram of X-ray transitions is illustrated in Figure 2.

$L\ell$  -emission is originated the transition between  $L_3$  and  $M_1$ . Since  $M_1$  shell of Ti is a closed shell, Ti- $L\ell$  emission does not have the chemical bonding information. On the other hand,  $L\alpha,\beta$  emissions are originated the transition between  $L_{2,3}$  and  $M_{4,5}$ . In the case of Ti, the  $M_{4,5}$  shell are not fully occupied by the electrons and are the outermost shell (parts of valence bands). In NEXAFS and Valence-to-core X-ray emission spectroscopy (vtc-XES) analyses reported in the prior arts[25,26,30,31], Ti(2p) binding states and the transition state of Ti- $K\beta$ " and  $K\beta_{2,5}$  (the X-ray is generated from valence band;  $N_2(4p_{1/2})$ ,  $N_4(4d_{3/2})$ ,  $M_4(3d_{5/2})$  and  $N_3(4p_{3/2})$ ,  $M_5(3d_{5/2})$  to core  $K(1s)$ ) were tracked. In our report, Ti- $L\alpha\beta$  was used to observe the transition state from the valence band;  $M_{4,5}(3d_{5/2}, 3/2)$  to  $L_{2,3}(2p_{1/2}, 2p_{3/2})$ . In these case,  $K(s)$  and  $L_{2,3}(2p_{1/2}, 2p_{3/2})$  are relatively stable and sharp energy. However, the valence band is more sensitive for the chemical bonding of solid states than the inner shell energy such as  $K(1s)$  and  $L_{2,3}(2p_{1/2}, 2p_{3/2})$ .

Based on these considerations, we analyzed the Ti  $L\alpha,\beta$  emissions.

Regarding Mg  $K\alpha$  (3rd order) shown in Figure 3, this is known as higher order X-rays, which observed at 3 times wavelength (1/3 times energy) of 1st order X-ray. That is, Mg  $K\alpha$  (1st order) is 1253.6 eV (Figure 1), but the spectrum is also visible at around 418 eV which is Mg- $K\alpha$  (3rd order).

As mentioned above, we have described the signal assignments appearing in the SXES measurement chart of  $MgCl_2$ -supported catalysts and the effectiveness of using Ti  $L\alpha,\beta$  emissions for evaluation of Ti's outermost shell electrons. In order to obtain even more quantitative information, a method for evaluating Ti  $L\alpha,\beta$  emission signals will be further described.

In previous reports, we have analyzed the ratio of the peak heights of 452.0 eV on the low energy side and 458.0 eV on the high energy side. The signals appearing in the energy region from 420.0 eV to 490.0 eV, in which Ti  $L\alpha,\beta$  are included, needs to be divided to two energy area as the representatives of low energy and high energy.

Therefore, the next step is to set the thresholds. To determine the separation point of X-ray energy two materials, 48h co-grinded products of  $MgCl_2$  and  $TiCl_4$  and  $TiCl_4/DBP$  complexes were used [40,41]. SXES measurements of these two materials. The SXES spectrum is shown in Figure 4.

In  $TiCl_4/DBP$  complex that show little polymerization activity, the SXES signal on the low-energy side is strongly expressed. We have reported that the electron density of Ti in  $TiCl_4/DBP$  complex shall be reduced by the ionic characteristics between Ti and COOR interaction [11,24,27,29,40]. Accordingly, the SXES signal of low energy region is implied to the Ti species



having relatively low activity.

On the other hand, the polymerization activity of  $\text{MgCl}_2$  and  $\text{TiCl}_4$  48h co-grinded product is enough high and the SXES signal on the relatively high energy side is greatly displayed. Considering the relationship between the polymerization activity and the X-ray energy in SXES, we decided that the signal intensity area between 438.0 eV to 455.0 eV was classified as low energy and that between 455.1 eV to 470.0 eV was as high energy, respectively.

Using the analysis method described above, SXES analysis was performed on three  $\text{MgCl}_2$ -supported catalysts (Cat.A, B, and C) and  $\text{TiCl}_3$  catalysts for comparison. Table 1 summarizes the evaluation results of SXES and propylene polymerization. And SXES spectra are shown in Figures 5 to 9.

As shown in Table 1, LE/HE ratio value of  $\text{TiCl}_3$  catalyst was quite higher than those of  $\text{MgCl}_2$  supported catalysts. The relatively large number of LE/HE of  $\text{TiCl}_3$  catalyst. Figure 5 is the comparison of SXES charts of  $\text{TiCl}_3$  and  $\text{MgCl}_2$  supported one (Cat.C). It could be confirmed that  $\text{MgCl}_2$ -supported catalyst showed the strong signal at high energy side.

The effect of triethylaluminium treatment of  $\text{MgCl}_2$  supported catalyst on SXES signal change was investigated. As shown in Table 1, it was found that the ratio of the high-energy side increased when the catalyst contacted with triethylaluminium. This behavior was seemed to be universal among the three kinds of catalyst. Since the triethylaluminium treatment of catalyst eliminates the inert (weakly supported) Ti atoms from  $\text{MgCl}_2$  surface (Table 1), the smaller values of LE/HE after triethylaluminium treatments in Table 1 strongly indicates that the active Ti shows the polarization of higher energy side of Ti  $L_{\alpha,\beta}$  in SXES. This may be due to interactions with other elements in the vicinity, which may have altered the electronic structure of Ti.

From the polymerization activity data listed in Table 1, it should notice that the catalytic activity was almost maintained even after the triethylaluminium treatment. This clearly indicates that the heptane washing of the triethylaluminium treatment of the solid is effective to remove the remaining free triethylaluminium to minimize the chemical alternation of the solid such as over-reduction of Ti.

Also, low temperature storage of the triethylaluminium treated solid should avoid thermal decomposition of the solid. It shall vary assure that SXES results of the triethylaluminium treated solids are strongly reflecting the nature of active titanium species on the solid surface.

Figure10 is the parts of the catalytic activity against  $\text{HE}/(\text{HE}+\text{LE})$  values obtained by SXES measurements by using the data listed in Table1.

As mentioned before, the activity level was almost no change by triethylaluminum treatment. But  $\text{HE}/(\text{HE}+\text{LE})$  value was clearly sifted toward to higher range.

Taking into account of the Ti content reduction by triethylaluminum treatment shown in Table1, it can be concluded that the SXES results of triethylaluminum treated solid provides the important spectroscopic information of active Ti atoms.



This phenomenon is corresponding to the understanding reported in the prior arts [6,11,13,17,40,41,42].

We reported on the electron density and activity of Ti using high-field solid-state NMR, and in this case, the polymerization activity also improves as the electron density of Ti increases. In this case, it was concluded that the electron density of Ti increased due to the flow of electrons from Mg to Ti, which was consistent with the DFT calculation results [6,27]. In the case of SXES, as in NMR[6,17,18,29], the electrons flow from Mg to Ti via Cl takes place due to low electronegativity of Mg, resulting in the high electron density of Ti. The high electron density of active Ti shall be lower the energy level of coordinated monomer by the strong back donation from d-electron of Ti to  $\pi^*$  orbital to coordinated olefin monomer. The stable monomer adsorption drops the activation energy of successive monomer insertion step in the coordination polymerization mechanism [11,40].

In conclusion, Ti-L $\alpha,\beta$  SXES analysis of triethylaluminium activated MgCl<sub>2</sub> supported TiCl<sub>4</sub> catalysts conducted in present work could obtain the chemical bonding state of Ti in the catalyst, probably supporting to the past hypothesis to understand the high activity of MgCl<sub>2</sub> supported Ziegler-Natta catalyst.

## CONCLUSION

The state of the outermost shell electrons of Ti atoms in propylene polymerization catalysts was analyzed using a small SXES instrument developed by JEOL. Although the resolution was not necessarily high, the difference in catalytic activity could be confirmed as a difference in spectra. That is, the catalytic activity was correlated with the intensity ratio between low and high signals of Ti in SXES measurement. And in the case of the strong intensity of high energy side signal, it showed high catalytic activity.

The triethylaluminium treatment of MgCl<sub>2</sub> supported catalyst induced the Ti element extraction from the solid, resulting in that the strong energy signal intensity was relatively enhanced.

Considering the solid <sup>13</sup>C-NMR analyses data of the Ziegler-Natta catalyst described in our previous report, the polarization of high energy side signal of Ti L $\alpha,\beta$  in SXES results seemed to be relation with the NMR results for carbonyl function[6,17,29].

The validity of this work results shall be ensured in detail with high-resolution SXES using a synchrotron. In addition, the effects of the polymerization conditions such as temperature and external donor (stereospecificity control reagent of polypropylene) addition on the active Ti properties shall need to be examined by SXES for deeper understanding of working state of the catalyst.

## ACKNOWLEDGEMENT

We would like to express our appreciation to Mr. Osamu Emura, Mr. Keiji Tochigi, Dr. Shougo Koshiya, Mr. Takeshi Takeuchi, Dr. Koji Yazawa, Mr. Kenichi Tsutsumi, Mr. Keiichiro Hosaka, Mr. Hiromichi Tanaka and Ms. Maki Sonobe of JEOL Ltd., and Dr. Michiaki Adachi of Toho Titanium Co., Ltd. for their cooperation in this study.

## REFERENCES

1. Ziegler K, Holzkamp E, Breil H, Martin H (1955) Das mülheimer normaldruck-polyäthylen-verfahren. *Angew Chem* 67: 541-547 [\[CrossRef\]](#)
2. Natta G (1955) Une nouvelle classe de polymeres d'  $\alpha$ -olefines ayant une régularité de structure exceptionnelle. *J Polym Sci* 16:143-154 [\[CrossRef\]](#)
3. Natta G (1956) Stereospezifische katalysen und isotaktische polymere. *Angew chem* 68: 393-403 [\[CrossRef\]](#)
4. Kashiwa N (1980) Super active catalyst for olefin polymerization. *Polym J* 12:603-608 [\[CrossRef\]](#)
5. Toyota A, Kashiwa N(1981) Method for producing high-performance supported catalyst component, Jap Patent:1,014,471
6. Ohashi R, Saito M, Fujita F, Nakai T, Utsumi H, Deguchi K, Tansho M, Shimizu T (2012) Observation of  $^{47,49}\text{Ti}$  NMR Spectra of  $\text{TiCl}_4/\text{MgCl}_2$  catalysts under an ultrahigh magnetic field. *Chem Lett* 41:1563-1565 [\[CrossRef\]](#)
7. Brevard G (1981) Handbook of high resolution multinuclear NMR, John Wiley & Sons, Fig. 23, pp.56
8. Laszlo P (1983) NMR of newly accessible nuclei, Academic Press, New York, pp.1, 18
9. Drakenberg T, Forsen S (1983) The alkaline earth metals biological applications. In: The multinuclear approach to NMR spectroscopy, eds: J. B. Lambert, F. G. Riddell, pp.309
10. Keii T, Suzuki E, Tamura M, Murata M, Doi Y (1982) Propene polymerization with a magnesium chloride-supported Ziegler catalyst, 1. principal kinetics. *Makromol Chem* 183: 2285-2304 [\[CrossRef\]](#)
11. Doi Y, Soga K, Murata M, Suzuki E, Ono Y, Keii T (1983) Additive effect of metal chlorides on propylene polymerization with a soluble titanium-based Ziegler catalyst. *Polym Commun* 24: 244-246 [\[CrossRef\]](#)
12. Terano M, Kataoka T, Keii T (1986) Analysis of  $\text{MgCl}_2$ -supported high-yield catalysts by thermal analysis and infrared spectroscopy. *Macromol Chem Rapid Commun* 7: 725-731 [\[CrossRef\]](#)
13. Kakugo M, Miyatake T, Naito Y, Mizunuma K (1988) Microtacticity distribution of

- polypropylenes prepared with heterogeneous Ziegler-Natta catalysts. *Macromolecules* 21: 314-319 [\[CrossRef\]](#)
14. Terano T, Kataoka T, Keii T (1987) A study on the states of ethyl benzoate and  $\text{TiCl}_4$  in  $\text{MgCl}_2$ -supported high-yield catalysts. *Makromol Chem* 188: 1477-1487 [\[CrossRef\]](#)
  15. Abis L, Albizzati E, Giannini U, Giunchi G, Santoro E, Noristi L (1988) Cross polarization/magic angle spinning  $^{13}\text{C}$  solid state nuclear magnetic resonance of model compounds related to supported Ziegler-Natta catalysts. *Makromol Chem* 189: 1595-1601 [\[CrossRef\]](#)
  16. Sormunen P, Hjertberg T, Iiskora E (1990) A solid-state  $^{13}\text{C}$  NMR study on heterogeneous Ziegler-Natta catalyst components. *Makromol Chem* 191: 2663-2673 [\[CrossRef\]](#)
  17. Terano M, Saito M, Kataoka T (1992) Solid-state  $^{13}\text{C}$  NMR study on the state of the electron donor in  $\text{MgCl}_2$ -supported catalysts. *Makromol Chem Rapid Commun* 13: 103-108 [\[CrossRef\]](#)
  18. Härkönen M, Seppälä JV, Chûjô R, Kogure Y (1995) External silane donors in Ziegler-Natta catalysis: A two-site model simulation of the effects of various alkoxysilane compounds. *Polymer* 36:1499-1505 [\[CrossRef\]](#)
  19. Bahri-Laleh N, Nekoomanesh-Haghighi M, Mirmohammadi SA (2012) A DFT study on the effect of hydrogen in ethylene and propylene polymerization using a Ti-based heterogeneous Ziegler-Natta catalyst. *J Organomet Chem* 719: 74-79 [\[CrossRef\]](#)
  20. Bahri-Laleh N, Hanifpour A, Mirmohammadi SA, Poater A, Nekoomanesh-Haghighi M, Talarico G, Cavallo L (2018) Computational modeling of heterogeneous Ziegler-Natta catalysts for olefins polymerization. *Prog Polym Sci* 84: 89-114 [\[CrossRef\]](#)
  21. Zohuri GH, Askari M, Ahmadjo S, Damavandi S, Eftekhar M, Bonakdar MA (2010) Preparation of ultra-high-molecular-weight polyethylene and its morphological study with a heterogeneous Ziegler-Natta catalyst. *J Appl Polym Sci* 118: 3333-3339 [\[CrossRef\]](#)
  22. Jamjah R, Zohuri G H, JVaezi J, Ahmadjo S, Nekomanesh M, Pouryari M (2006) Morphological study of spherical  $\text{MgCl}_2 \cdot n\text{EtOH}$  supported  $\text{TiCl}_4$  Ziegler-Natta catalyst for polymerization of ethylene. *J Appl Polym Sci* 101: 3829-3834 [\[CrossRef\]](#)
  23. Zohuri G H, Jamjah R, Ahmadjo S (2006) Comparative study of propylene polymerization using monosupported and bisupported titanium-based Ziegler-Natta catalysts. *J Appl Polym Sci* 100: 2220-2226 [\[CrossRef\]](#)
  24. Saito M, Uozumi T, Sugano T, Kataoka T, Chujo R (2018) Correlation between catalyst performance and relaxation time of electron donor in olefin polymerization catalyst by solid  $^{13}\text{C}$  NMR. *Kobunshi Ronbunshu* 75: 570-575 [\[CrossRef\]](#)
  25. Groppo E, Gallo E, Seenivasan K, Lomachenko K, Sommazzi A, Bordiga S, Glatzel P, Silfhout RV, Kachatkou A, Bras W, Lamberti C (2015) XAS and XES techniques shed light on the dark side of Ziegler-Natta catalysts: Active-site generation. *Chem Cat Chem* 7: 1432-1437 [\[CrossRef\]](#)

26. Taniike T, Terano M (2018) High-precision molecular modelling for Ziegler-Natta catalysts. *J Japan Petrol Ins* 61: 182-190 [\[CrossRef\]](#)
27. Iijima T, Shimizu T, Goto A, Deguchi K, Nakai T, Ohashi R, Saito M (2019)  $^{47,49}\text{Ti}$  Solid-state NMR and DFT study of Ziegler-Natta catalyst: Adsorption of  $\text{TiCl}_4$  molecule onto the surface of  $\text{MgCl}_2$ . *J Phys Chem solids* 135:109088 [\[CrossRef\]](#)
28. Piovano P, Signorile M, Signorile M, Torelli P, Martini A, Martini A, Takasao G, Taniike T, Groppo E (2021) Electronic properties of Ti sites in Ziegler–Natta catalysts. *ACS Catal* 11: 9949-9961 [\[CrossRef\]](#)
29. Saito M, Uozumi T, Murata M, Kataoka T, Chujo R (2022) Characterization of phthalate internal donor in  $\text{MgCl}_2$  supported Ziegler-Natta catalyst by solid state  $^{13}\text{C}$  NMR. *Polyolefins J* 9: 117-127 [\[CrossRef\]](#)
30. Chikuma H, Takasao G, Wada T, Chammingkwan P, Behler J, Taniike T (2023) Accelerating non-empirical structure determination of Ziegler–Natta catalysts with a high-dimensional neural network potential. *J Phys Chem C* 127: 11683-11691 [\[CrossRef\]](#)
31. Zarupski J, Piovano A, Signorile M, Amodio A, Olivi L, Hendriksen C, Friederichs N H, Groppo E (2023) Silica-magnesium-titanium Ziegler-Natta catalysts. Part1: Structure of the pre-catalyst at a molecular level. *J Catal* 424: 236-245 [\[CrossRef\]](#)
32. Terauchi M, Yamamoto H and Tanaka, M (2001) Development of a sub-eV resolution soft-X-ray spectrometer for a transmission electron microscope. *J Electron Microsc* 50: 101-104 [\[CrossRef\]](#)
33. Terauchi M, Takahashi H, Handa N, Murano T, Koike M, Kawachi T, Imazono T, Koeda M, Nagano T, Sasai H, Oue Y, Yonezawa Z, Kuramoto S (2012) Ultrasoft-X-ray emission spectroscopy using a newly designed wavelength-dispersive spectrometer attached to a transmission electron microscope. *J Electron Microsc* 61: 1-8 [\[CrossRef\]](#)
34. Takakura M, Murano T, Takahashi H (2015) Newly Developed Soft X-ray Emission Spectrometer, SS94000SXES, *JEOL News* 50: 64-68 [\[CrossRef\]](#)
35. Terauchi M, Koshiya S, Kimoto K (2017) Information observed in  $\text{Ti-L}_{\alpha,\beta}$  and  $\text{Ti-L}_{1,\eta}$  emission lines of Ti and its oxides. *IOP Conf Series: Mater Sci Eng* 304: 012018-1-6 [\[CrossRef\]](#)
36. Terauchi T, Sato Y (2018) Chemical state analyses by soft X-ray emission spectroscopy. *JEOL NEWS* 53: 30-35 [\[CrossRef\]](#)
37. Takahashi H, Murano T, Takakura M, Asahina S, Terauchi M, Koike M, Imazono T, Koeda M, Nagano T (2018) Development of soft X-ray emission spectrometer for EPMA/SEM and its application. *IOP Conf Ser Mater Sci Eng* [\[CrossRef\]](#)
38. Sakuda Y, Ishizaki M, Togashi T, Asahina S, Takakura M, Takahashi H, Kurihara M (2016) Chemical state analysis using Soft X-ray Emission Spectrometry in low voltage FE-SEM. *European Microscopy Congress 2016: Proceedings* [\[CrossRef\]](#)
39. Bearden JA (1967) X-Ray Wavelengths. *Rev Mod Phys* 39: 78 [\[CrossRef\]](#)

40. Saito M, Murata M, Kataoka T, Sakuda Y, Takahashi H (2022) Characterization of electronic properties of titanium atom in heterogeneous Ziegler-Natta catalyst analyzed by soft X-ray emission spectrometry (SXES). *Bull Chem Soc Jpn* 95: 367-373 [\[CrossRef\]](#)
41. Saito M, Kataoka T, Murata M, Nakajima Y, Masuko R, Yamada H, Takahashi H (2023) Advanced analytical methods for the evaluations of olefin polymerization catalysts and produced polymers. *JEOL News* 58: 27-34 [\[CrossRef\]](#)
42. Wada T, Thakur A, Chammingkwan, Terano M, Taniike T, Piovano A, Groppo E (2020) Structural disorder of mechanically activated  $\delta$ -MgCl<sub>2</sub> studied by synchrotron X-ray total scattering and vibrational spectroscopy. *Catalysts* 10: 1089-1103 [\[CrossRef\]](#)

**Table 1.** Results of catalyst solid characterizations and propylene polymerization tests.

Compound	Ti <sup>(b)</sup> (wt%)	SXES <sup>(c)</sup> Results HE/((LE+HE) <sup>(d)</sup>	Activity <sup>(e)</sup> g-PP/g-catalyst	HY <sup>(f)</sup> %
Cat.A	2.5	0.357	6,000	95.8
Cat.B	1.3	0.365	13,000	96.0
Cat.c	2.1	0.377	26,900	96.9
Cat.A(Al) <sup>(a)</sup>	0.5	0.368	5,650	95.7
Cat.B(Al) <sup>(a)</sup>	0.2	0.380	12,500	95.9
Cat.C(Al) <sup>(a)</sup>	0.4	0.386	24,200	96.7
TiCl <sub>3</sub>	23	2.680	50	85.0

<sup>(a)</sup>Triethylaluminum contact.

<sup>(b)</sup>Determined by UV.

<sup>(c)</sup>SXES: Soft X-ray Emission Spectrometer.

<sup>(d)</sup>HE: High Energy(455.1eV to 470.0eV),LE: Low Energy (438.0eV to 455.0eV)

<sup>(e)</sup>Bulk Polymerization.

<sup>(f)</sup>Heptane insoluble.

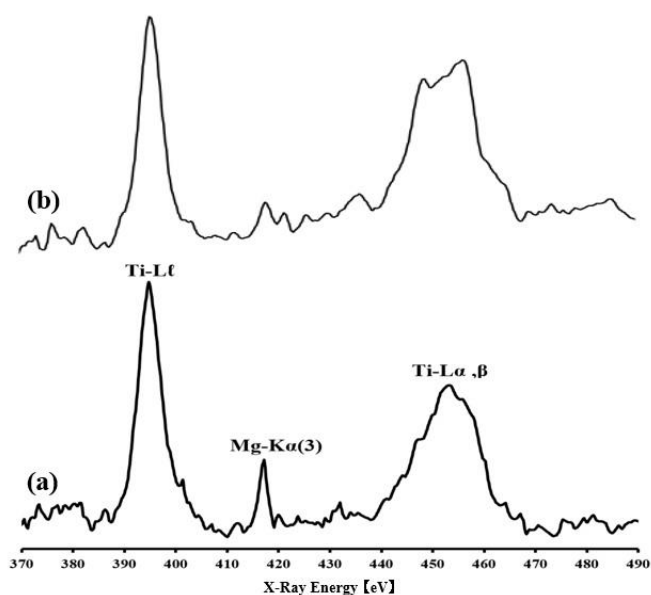


**Figure 1.** Ti L and  $L_{\alpha,\beta}$  emission SXES spectra of  $MgCl_2$ -supported catalyst, (a) before contact with triethylaluminum, (b) after contact with triethylaluminum.

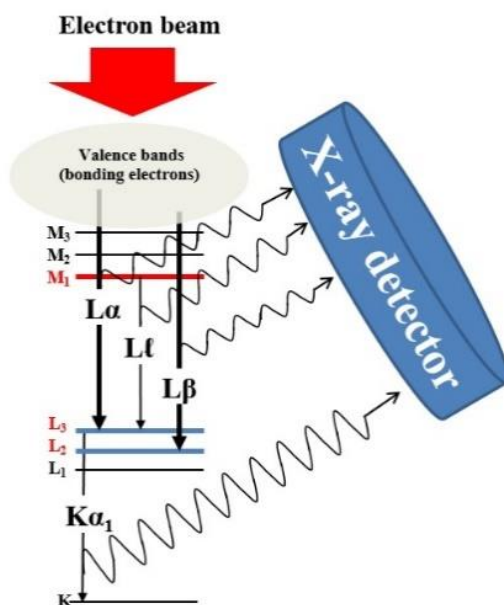


**Figure 2.** Schematic diagram of characteristic X-ray emission and detection.

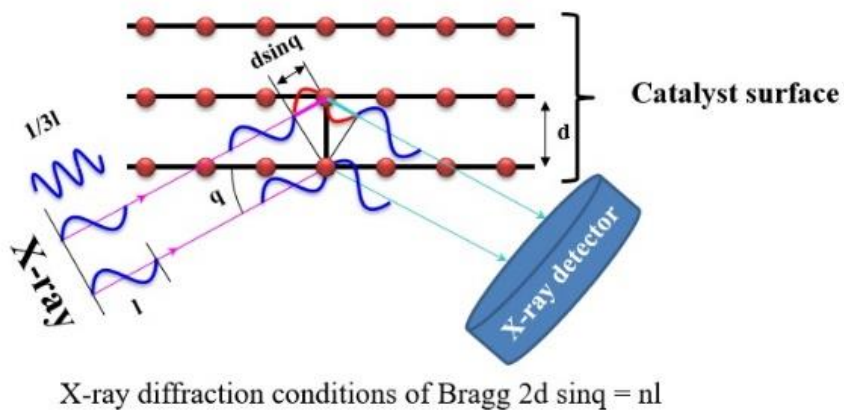


**Figure 3.** Schematic illustration of Mg-K emission 3rd order by Bragg x-ray diffraction.

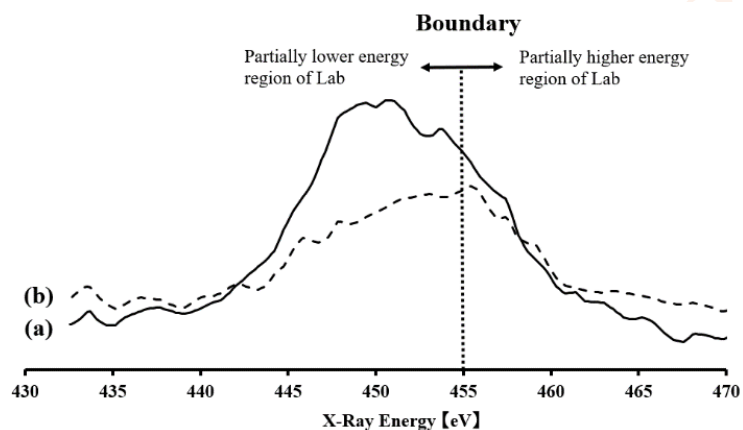


**Figure 4.** Determining base values for SXES spectra:(a)  $\text{TiCl}_4$  DBP complexes, (b)  $\text{MgCl}_2/\text{TiCl}_4$  48h co-grinded catalyst.

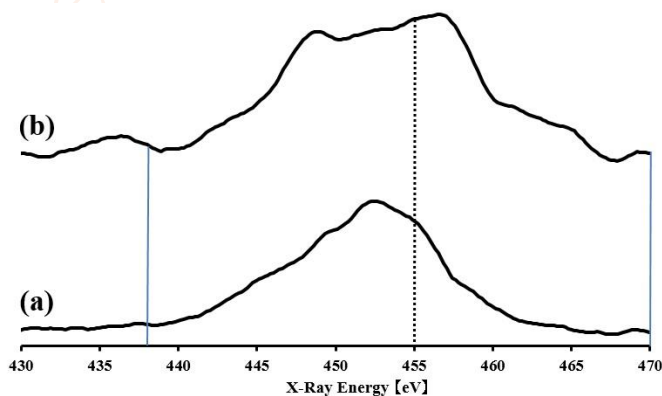


**Figure 5.** Ti  $L_{\alpha,\beta}$  emission SXES spectra of  $\text{TiCl}_3$  catalyst and after triethylaluminum Cat.C type catalyst by SXES:(a)  $\text{TiCl}_3$  catalyst,(b) Cat.C Type catalyst.



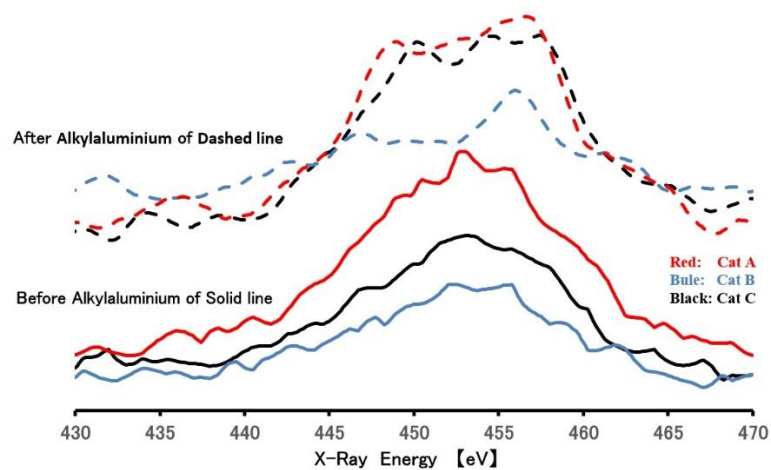


**Figure 6.** Ti  $L_{\alpha,\beta}$  emission SXES spectra in  $MgCl_2$ -supported catalyst before and after triethylaluminum contact. (Red) Cat A type catalyst, (Blue) Cat B type catalyst, (Black) Cat C type catalyst.

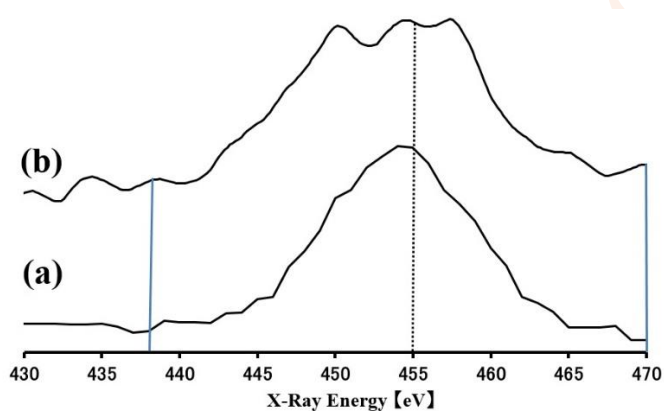


**Figure 7.** Ti  $L_{\alpha,\beta}$  emission SXES spectra of Cat.A by SXES: (a) before triethylaluminum, (b) after triethylaluminum.

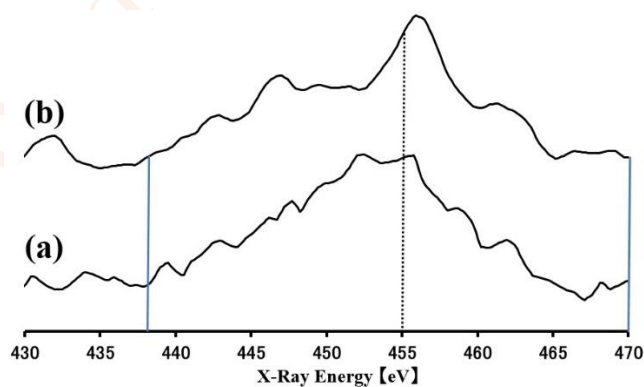


**Figure 8.** Ti  $L_{\alpha,\beta}$  emission SXES spectra of Cat.B by SXES: (a) before triethylaluminum, (b) after triethylaluminum.

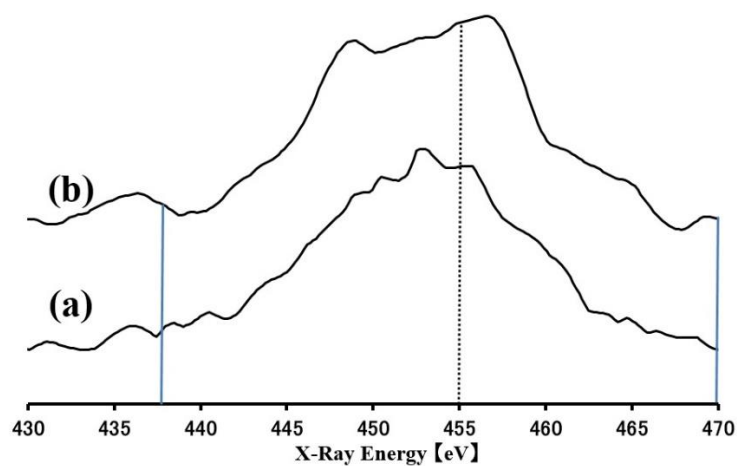


**Figure 9.** Ti L $\alpha,\beta$  emission SXES spectra of Cat. C by SXES. (a) before triethylaluminum, (b) after triethylaluminum.

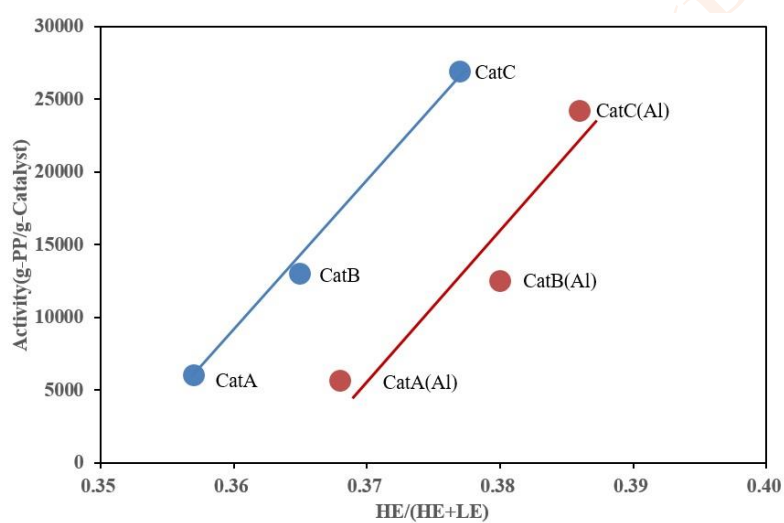


**Figure 10.** Relationships between HE/(HE+LE) values determined by SXES and propylene polymerization activity, (Blue) before triethylaluminum treatment, (Red) after triethylaluminum treatment.